ISSN: 2349-5197
Impact Factor: 2.715

INTERNATIONAL JOURNAL OF RESEARCH SCIENCE & MANAGEMENT

INDENTATION OF SANDWICHES USING A LAYERWISE MODEL WITH FIXED DEGREES OF FREEDOM

Ugo Icardi*[1] and Andrea Urraci[2]
*1&2Dipartimento di Ingegneria Meccanica e Aerospaziale, Politecnico di Torino, Italy

DOI: 10.5281/zenodo.572574

Keywords: Sandwich indentation, core crushing, mesoscale damage model, hierarchic representation, variable kinematics,

Abstract
A zig-zag plate model with variable kinematics and fixed degrees of freedom recently developed by the authors is applied to study indentation of sandwiches with honeycomb/foam core, with the aim of reducing the computational burden. This model, which *a priori* fulfils the stresses and displacements continuity requirements, has a hierarchic representation of displacements, but just five degrees of freedom. The core crushing behaviour is determined apart once at a time in order to account for the variable elastic properties of the core during the structural analysis. Specifically, shell elements with elastic-plastic isotropic material are adopted to discretize the cellular structure and the faces, instead solid elements with nonlinear material behaviour are chosen to model foams. Once the properties of core are determined, the analysis is quickly carried out in closed form by the zig-zag model. As customarily, the onset of damage is determined using stress based criteria, while its growth is accurately and efficiently described using a mesoscale model. In this way, the degraded properties of the failed regions are evaluated with a physically based model, instead of guessing suited multiplication factors. The numerical results of simulations are shown to be in good agreement with experiments taken from the literature.

Introduction
The continuous quest for lighter and stronger structures has favoured the spread of sandwiches with laminated faces in the aerospace industry and in many other engineering applications. However, a full exploitation of the advantages offered by these materials (low weight, excellent strength, stiffness, energy absorption and fatigue properties) requires an accurate modelling of local effects in the microstructure. Attention has to be paid to the local damage rise and growth in service, due to the inability of sandwiches to yield and dissipate a large amount of energy via plasticity. This topic is thoroughly discussed in the book by Daniel and Ishai [1] and in the recent papers by Davies et al. [2] and de Freitas et al. [3].

The general agreement is that parameters such as distribution, magnitude and duration of stresses, load history, stacking sequence, strengths and pre-existing defects have a significant bearing on damage nature, position and extent. It is commoly accepted that the damage of sandwiches is dominated by the crushing of core followed by tearing of the loaded face. Parameters such as topology of cells, their relative density and the thickness of the foil strongly affect this phenomenon. Instead, the damage of laminated faces begins as matrix cracking, fibres breakage and local puncture. Then, when cracks reach an interface and deflect onto it, delamination develops.
Beside these aspects, it is well known that an accurate simulation of the mechanisms of damage initiation and growth is mandatory in order to properly design damage tolerance structures. In this context, it is clear that the computational burden is strongly affected by the efficiency of the structural model.

Great attention should be paid to the analysis of indentation (i.e. low-velocity impact), since it can produce barely visible damages, which have a significant influence on the structural performance and the service life. Indentation is often studied using three-dimensional (3-D) finite element analyses (FEA) and fracture mechanics or cohesive zone models (see, e.g. Wang et al. [4], Borg et al. [5] and Nishikawa et al. [6]). In this way, accurate results are obtained, though at the expense of a high computational effort. The analysis has been also successfully performed using high order layerwise (HLW) models, or even less refined plate models as structural models, stress-based failure criteria to determine the onset of damage and multiplication factors that

degrade the elastic properties for describing the damage growth (see, e.g. Diaz-Diaz et al. [7] and Qiao and Yang [8]).
Here, we follow this latter approach, because we use our recently developed zig-zag model with variable kinematics and fixed degrees of freedom (d.o.f.) that is referred as FD_VK [9]. This model has the merit of obtaining numerical results as accurate as 3D model directly from constitutive equations, though only 5 functional d.o.f. are employed like in the equivalent single layers models. Differently to what done in the previous works [9] and [10], in this paper a reduced order of expansion and an increased number of computational layers are used, since numerical tests have proven this approach to be more efficient for sandwiches. This choice does not result into a larger computational effort, because irrespective of the used number of computational layers, the number of d.o.f. is fixed.

Being a homogenized model, the FD_VK cannot properly treat crushing of soft cores, as it highly depends on geometry and material properties. To keep low the computational effort, the crushing behaviour is evaluated apart once at a time. The variable, apparent elastic properties of core under compressive loading are determined through a detailed 3D finite element analysis. Specifically, plate elements are used to discretize the face sheets and the cellular structure of honeycomb, while foam core is discretized by solid elements with non-linear material behaviour.

The computational burden is kept as low as possible, since after having determined the properties of core, the analysis is carried out in closed form by the FD_VK model. As the core crushing behaviour is determined apart and the FD_VK model has very low computational costs, the indentation analysis is consistently speeded-up, thus enabling to study structures of industrial complexity.

However, at the same time, this approach can describe the most significant local phenomena, because the properties are assumed to vary with the applied load and from the points over the contact area to the neighbouring points, according to the results by the detailed finite element analysis.

As customarily, the onset of damage is predicted with stress-based criteria, on the contrary, the damage growth is described using the mesomechanic model by Ladevèze et al. [11]-[12], which considers the effects of the damage on the microscale through a modified expression of the strain energy. The progressive failure analysis is performed extending a pre-existing damage to the points where the ultimate condition is reached, as predicted by the criteria. The mesomechanic model is chosen because, as explained in [13], this kind of models provides greater accuracy and smaller computational burden than structural scale models, which consider cracks as hard discontinuities.

Even if many authors agree that indentations can be studied using just static simulations, here a dynamic solver is developed that can treat general transient dynamic problems of practical interest, such as blast pulse loading or impacts. It is based on the Newmark's implicit time integration scheme, since this method does not require extremely small time steps to be stable and to limit convergence and rounding errors. However, in all the sample cases, numerical tests have shown that the dynamic effects on the average value of displacement are negligible, as expected. The indentation depth and the contact area are computed assuming the distribution of the contact force to be Hertzian and the projectile as a rigid body. At any time step, the iterative algorithm by Palazotto et al. [14] provides the contact area, forcing the surface of the target to conform the shape of the impactor, as required by soft media.

In the next section a brief overview about the main features and assumptions of the FD_VK structural model are presented. Then, the simulation procedure for describing the core crushing behaviour is explained and assessed. Next, the methods adopted to compute the damage indicators and the contact force are briefly reviewed. Finally, applications are presented, comparing the results by the simulation procedure presented to experiments available in literature.

Structural model

To sum up, the structural models should fulfil the contact conditions at the interfaces, in order to correctly describe the layerwise effects, as extensively discussed by Zhang and Yang [15], who reviewed HLW models.

Accordingly, the displacements should be continuous across the thickness, but their derivatives should be discontinuous at the material interfaces to make continuous the transverse shear and normal stresses at the layer interfaces, as prescribed by the elasticity theory. Furthermore, the models should satisfy the other constraints prescribed by the theory of elasticity (i.e. the stress-free boundary conditions at the upper and lower bounding faces). There are other important general aspects that should be fulfilled by the models. In fact, in order to respect the 3D solution, the same order of polynomials cannot be used for all the displacements and for any point across the thickness. In addition, the order of representation of each displacement should vary with the type of loading, the boundary conditions, the thickness ratio, the constituent materials and whether cylindrical or bi-directional flexure are considered, or else results could be inaccurate. Trying to reach a compromise between accuracy and computational costs saving, many models have been developed that fully or partially satisfy these requirements.

At the present, the best available models in coupling accuracy and efficiency are HLW. They can be classified as models with a number of functional d.o.f. that depends on the number of physical layers (see, e.g., Moreira and Rodrigues [16], Chrysochoidis and Saravanos [17], Hohe and Librescu [18], and Shariyat [19]) and models with a fixed number of d.o.f. (see, e.g., the zig-zag models by Icardi and Sola [9] and Zhen and Wanji [20]). The former approach is easier to develop, since complex algebraic manipulations are not required, however accurate estimates are achieved at the expense of a high computational burden. Instead, the zig-zag models require a higher effort during their development in order to derive the expression of all the unknowns as function of the d.o.f. However this operation can be carried out apart once at a time, thus consistently speeding-up the analysis, as shown in [9]. This aspect fosters the application of HLW models with fixed d.o.f. to the analysis of structures of industrial complexity and of highly iterative problems, such as impacts.

Notation

The structures are referred to a rectangular Cartesian reference frame (x, y, z) placed on their middle plane Ω, with z normal to Ω, and x, y on Ω. The symbols $^{(k)}z^{+}$ and $^{(k)}z^{-}$ indicate the position of the upper^{+} and lower $^{-}$ surfaces of the kth layer, the quantities that belong to a generic layer k are denoted with the superscript $^{(k)}$. The symbols u, v, w represent respectively the elastic displacements in the direction of x, y and z.

The FD_VK structural model

The through-the-thickness variation of the displacements is postulated in the following general, piecewise form [9]:

$$u(x,y,z) = U^0(x,y,z) + U^i(x,y,z) + U^c(x,y,z) \quad (1)$$

$$v(x,y,z) = V^0(x,y,z) + V^i(x,y,z) + V^c(x,y,z) \quad (2)$$

$$w(x,y,z) = W^0(x,y,z) + W^i(x,y,z) + W^c(x,y,z) \quad (3)$$

The symbols with the superscript 0 represent the contributions that are fixed in all the layers, those with the superscript i are the terms that vary between the different layers and finally the superscript c characterizes the contributions that enable to fulfil the continuity conditions prescribed by the elasticity theory. The explicit expressions of the fixed terms are:

$$U^0(x,y,z) = u^0(x,y) + z(\gamma_x^0(x,y) - w^0{}_{,x}) \quad (4)$$

$$V^0(x,y,z) = v^0(x,y) + z(\gamma_y^0(x,y) - w^0{}_{,y}) \quad (5)$$

$$W^0(x,y,z) = w^0(x,y) \quad (6)$$

Equations (4)-(6) just contain the in-plane displacements of the points over the middle plane $u^0(x,y)$, $v^0(x,y)$, the transverse displacement $w^0(x,y)$ and the shear rotations of the normal $\gamma_x^0(x,y)$, $\gamma_y^0(x,y)$ to these points. These quantities are the functional d.o.f.

The expression of the layers contributes is:

ISSN: 2349-5197
Impact Factor: 2.715

INTERNATIONAL JOURNAL OF RESEARCH SCIENCE & MANAGEMENT

$$U^i(x,y,z) = A_{x2}(x,y)z^2 + ... + A_{xn}(x,y)z^o \quad (7)$$

$$V^i(x,y,z) = A_{y2}(x,y)z^2 + ... + A_{yn}(x,y)z^o \quad (8)$$

$$W^i(x,y,z) = A_z(x,y)z + ... + A_{zn}(x,y)z^o \quad (9)$$

These terms are valid within a single layer of the structure; however the number of d.o.f. is fixed, since their expressions are computed apart as function of the d.o.f using a symbolic calculus tool. Their expression are obtained imposing the constraints prescribed by the elasticity theory (i.e. the stress-free boundary conditions at the upper and lower bounding faces) and the equilibrium conditions at $n_p = N_{lay} \cdot ord\_u - 2$ points across the thickness, N_{lay} being the number of computational layers and *ord_u* the chosen expansion order. The locations of the n_p points are picked arbitrarily, however they should not be placed excessively near to the interfaces in order to avoid singularity. By properly choosing the expansion order and the number of subdivision across the thickness, accurate predictions of the transverse shear and normal stresses are obtained directly from constitutive equations, even for thick structures with abruptly changing material properties.

Finally, the expressions of the terms that enable the fulfilment of the continuity constraints are:

$$U^c(x,y) = \sum_{k=1}^{n_i} \Phi_x^k(x,y)(z-z_k)H_k + \sum_{k=1}^{n_i} C_u^k(x,y)H_k \quad (10)$$

$$V^c(x,y) = \sum_{k=1}^{n_i} \Phi_y^k(x,y)(z-z_k)H_k + \sum_{k=1}^{n_i} C_v^k(x,y)H_k \quad (11)$$

$$W^c(x,y) = \sum_{k=1}^{n_i} \Psi^k(x,y)(z-z_k)H_k + \sum_{k=1}^{n_i} \Omega^k(x,y)(z-z_k)^2 H_k + \sum_{k=1}^{n_i} C_w^k(x,y)H_k \quad (12)$$

As prescribed by the elasticity theory for keeping equilibrium, the interlaminar stresses, the transverse normal stress and its gradient should be continuous at the interfaces. To this purpose, the expressions of Φ_x^k, Φ_y^k are obtained enforcing the continuity of the transverse shear stresses, while Ψ^k, Ω^k are obtained enforcing the continuity of the transverse normal stress and its gradient. Finally, C_u^k, C_v^k and C_w^k make continuous the displacements at the points across the thickness where the representation is varied. H_k is the Heaviside unit step function that activates the contribution of the continuity functions from the pertinent interface kth.

Similarly to what done for the high order terms, the explicit expressions of the continuity functions are derived in closed form using a symbolic calculus tool. As shown in [9], the closed-form expressions of high order terms and continuity functions involve the functional d.o.f. and their derivatives. As a consequence, when finite elements are developed, high-order shape functions and exotic nodal d.o.f. should be adopted. This drawback can be overcome with the strain energy updating technique (SEUPT) [21], which improves the accuracy of standard C^0 shear-deformable plate elements up to the level of the FD_VK model through fast post-processing operations.

Since all the sample cases considered in the numerical illustrations have simple geometry, loading and boundary conditions, the governing equations are solved using the Rayleigh-Ritz's method, assuming trigonometric expansions for the d.o.f.

The mass matrix is evaluated without introducing simplifying assumptions, because at certain frequencies the acceleration of the face sheets can be different from that of core, thus the higher order inertia terms do not always provide minor contributions. However, these effects are not relevant in the quasi-static sample cases considered in the numerical applications.

ISSN: 2349-5197
Impact Factor: 2.715

INTERNATIONAL JOURNAL OF RESEARCH SCIENCE & MANAGEMENT

Assessment of the FD_VK model

Assessments of the accuracy of the FD_VK model in describing the stress fields of sandwiches have been already presented in [9]. Here, as a further verification, let us consider the clamped sandwich square plate analysed by Ramtekkar et al. [22]. The material constituting the face sheets has the following mechanical properties: E_1=90,121 GPa, E_2= E_3=7,303 GPa, G_{12}= G_{13}=4,134 GPa, G_{23}=2,68 GPa, υ_{12}= υ_{13}=0,28, υ_{23}=0,34. The mechanical properties of the material constituting the core are: E_1= E_2= 0 GPa, E_3=2,076 GPa, G_{12}=0 GPa, G_{13}=0,358 GPa, G_{23}=0,122 GPa, υ_{12}= υ_{13}= υ_{23}=0. The stacking sequence is [0°/90°/core/0°/90°], the ratio between the thickness of the core and that of the faces is 8, while the length to thickness ratio S is 5. The stresses reported in Figure 1 are normalized as follow:

$$\bar{\sigma}_z = \frac{\sigma_z(0,0,z)}{p^0} \quad \bar{\sigma}_{xz} = \frac{\sigma_{xz}\left(-\frac{L_x}{2},0,z\right)}{p^0 S} \quad \bar{\sigma}_{yz} = \frac{\sigma_{xz}\left(0,-\frac{L_y}{2},z\right)}{p^0 S} \tag{13}$$

The symbol p^0 is the intensity of the uniformly distributed load. The comparison of the results by the FD_VK model with those obtained by Ramtekkar et al. [22] confirms the accuracy of the model. This case shows that the present model overtakes the drawbacks of the models with displacements and shear rotations as functional d.o.f., which often fail in the prediction of deflection and stresses in clamped components. In fact, it is sufficient to properly choose the trial functions, according to Chia [23]:

$$u^0(x,y) = \sum_{m=2,4}^{\infty}\sum_{n=1,3}^{\infty} A_{mn}\sin\left(\frac{m\pi x}{L_x}\right)\cos\left(\frac{n\pi y}{L_y}\right) \tag{14}$$

$$v^0(x,y) = \sum_{m=1,3}^{\infty}\sum_{n=2,4}^{\infty} B_{mn}\cos\left(\frac{m\pi x}{L_x}\right)\sin\left(\frac{n\pi y}{L_y}\right) \tag{15}$$

$$w^0(x,y) = \sum_{m=2,4}^{\infty}\sum_{n=2,4}^{\infty} C_{mn}\left[\cos\left(\frac{m\pi x}{L_x}\right)-(-1)^{m/2}\right]\left[\cos\left(\frac{n\pi y}{L_y}\right)-(-1)^{n/2}\right] \tag{16}$$

$$\gamma_x^0(x,y) = \sum_{m=2,4}^{\infty}\sum_{n=1,3}^{\infty} D_{mn}\sin\left(\frac{m\pi x}{L_x}\right)\cos\left(\frac{n\pi y}{L_y}\right) \tag{17}$$

$$\gamma_y^0(x,y) = \sum_{m=1,3}^{\infty}\sum_{n=2,4}^{\infty} E_{mn}\cos\left(\frac{m\pi x}{L_x}\right)\sin\left(\frac{n\pi y}{L_y}\right) \tag{18}$$

The numerical results of Figure 1 are obtained considering a third order expansion of the transverse displacement and a second order expansion of the in-plane displacements.

Please note that these trial functions are also adopted in the sample cases presented in the section Numerical results.

The crushing behaviour of soft cores

The soft material constituting the core of sandwiches plays an important role in determining the energy absorption of the structure. The typical behaviour is characterized by an initial linear phase at low strains, followed by a collapse phase, which finally turns into densification, as shown in many works taken from literature (see, e.g. Mohmmed et al. [24], Aminanda et al. [25], Aktay et al. [26], Flores-Johnson et al. [27] and Ivañez et al. [28]).

This behaviour is strongly affected by shear stress, because the ratio of this stress to other stresses determines the energy absorption of the core. Other general parameters that play an important role in determining the core crushing behaviour are the ratio of skin thickness to side length and the core density.

As far as simulation techniques are concerned, crushing is generally described through a detailed finite element simulation of the cellular structure of the honeycomb (Aminanda et al. [25] and Aktay et al. [26]), or using solid elements for foam core (Mohmmed et al. [24] and Ivañez et al. [28]). In details, honeycomb's cells are simulated using shell elements coupled with a self-contact algorithm that prevents from interpenetration between the folds in the cell walls. Instead, a proper modelling of foam core calls for the employment of suited homogenized material properties that are determined from experiments.

Of course, the refinement of the mesh used to discretize the soft core has an important role in describing the material behaviour. In fact, a coarse discretization determines a higher initial load peak and higher load in the densification regime. On the other hand, very refined mesh could be unsuited if the element size is not larger than the thickness of the honeycomb foil.

In order to keep the computational burden as low as possible, the soft material constituting the core can be treated as homogeneous material, according to Gibson and Ashby [29]. This approach was followed in previous works by the authors (see, e.g., [9] and [10]), since only the global response of the structure was required. Here the attention is focused on indentation, which instead needs to capture with the due accuracy all the local phenomena, such as the buckling of cell walls, in order to accurately describe the onset of damage and its growth. Accordingly, the apparent elastic moduli of the core while it collapses/buckles under transverse compressive loading are here determined with a detailed finite element analysis, which is performed apart once at a time. The evaluation of the elastic moduli is done in any sub-region in which the area around the contact point is discretized. Using the results by this analysis, the FD_VK model can then determine stress and displacement fields taking into consideration all the localized phenomena. In fact, though the core is treated as a homogeneous material by the FD_VK model, the effects of crushing are accounted for locally assuming elastic properties variable with position. The updated Lagrangian methodology is used, which evaluates the deformations at each new time step from the geometry of the structure at the previous step, not from the initial unloaded configuration. In this way, the nonlinear effects, considered when computing the apparent, variable elastic properties of the core, are accounted for during the structural analysis, even if the FD_VK model is based on infinitesimal strain-displacement relations. This methodology is chosen because it has an improved numerical efficiency than the standard Lagrangian approach, as claimed by Bathe [30].

With the above described simulation procedure, computational costs are reduced, since the detailed finite element analysis is limited to the preliminary phase, but, at the same time, accuracy is preserved, because the accuracy of the FD_VK model is similar to that of 3D models with a much lower computational effort.

During the preliminary finite element analysis used for predicting the core crushing behaviour, the honeycomb structure is described employing shell elements with elastic-plastic isotropic material, paying attention to adopt a self-contact algorithm to prevent from interpenetration of the folds in the cell walls. The cell walls bonded together are modelled using double shell elements. It is well known that compared to metallic core, Nomex™ honeycomb can present a relatively brittle behaviour, since fractures develop after reaching a critical load. Accordingly, in metallic honeycomb the collapse mechanism is plastic and starts after buckling, while Nomex™ honeycomb undergoes buckling of cells, followed by debonding failure at the cell interfaces and fracture. In order to capture this behaviour, failure criteria have been considered during the finite element analysis. Foam core is instead discretized using solid elements with nonlinear material behaviour, the properties being derived from experiments.

The finite element analysis is started below the lowest failure load predicted by the criteria of Lee and Tsotsis [31], Petras and Sutcliffe [32], Besant et al. [33], the rule suggested by Evonik for Rohacell foam, or the analytical model by Koissin et al. [34] for predicting wrinkling.

As an application, let us consider the Divinycell foam cores analysed by Flores-Johnson et al. [27]. Experiments were carried out in order to detect the crushing behaviour of two cubes with 25 mm edges in Divinycell H100 and H130 foams undergoing compressive load. Figure 2(a) reports the strain-stress behaviour for foam cores with different density, under uniaxial compression test. It could be noticed that the numerical results by the present model behave in accordance with the experimental ones.

As a further assessment we consider the experimental force-displacement curve detected by Aktay et al. [26] for an aluminium 5052 honeycomb with a density of 27 kg/m^3. The honeycomb has 6 cells in the width direction and 5 in the ribbon one, while its thickness is 50 mm. The cell side is 13,5 mm, while the cell wall thickness is 0,07 mm. Figure 2(b) shows the comparison between experimental and numerical results. Also in this case the simulation procedure provides satisfactory results.

Damage modelling

The damage in laminates begins as diffuse fibre-matrix debonding, whose accumulation determines transverse matrix microcracking. Their pattern is periodic, at least locally, and it is described in micromechanics by the cracking rate $\rho=L/H$ at the tip of cracks, L being the distance between two adjacent cracks and H being the length of the crack across the thickness. These microcracks determine at their tip a stress concentration, whose consequence is a degradation of the resin film between adjacent plies (i.e. the interface). The next step of the damage evolution is the growth of local cracks perpendicular to matrix microcracks (i.e. local delaminations) that, once coalesced under out-of-plane macroloading, turn into macroscopic interlaminar debonding. The pattern of local delamination cracks is also periodic, and it is quantified at each crack tip by the local delamination ratio $\tau=e/H$, where e is the length of the microcrack. It could be noticed that, according to experiments, the range of practical interest for ρ is [0; 0,7] and for τ is [0; 0,4], because for higher levels of degradation materials are fully damaged.

This micromechanical behaviour can be accurately described using fracture mechanic models, but at the expense of a high computational burden. To overcome this drawback, here the damage mesomodel (MSD) by Ladevèze et al. [11]-[12] is chosen, considering that this kind of models has an accuracy comparable to that of the above mentioned models, but an improved efficiency, as claimed by McQuigg [13].

The MSD easily describes the effects of damage, adopting an intermediate scale between the macroscale of the structure and the microscale of the damage mechanism. This method replaces the discretely damaged medium with a continuous homogeneous medium, equivalent from an energy standpoint and incorporating into the expression of the strain energy damage indicators. They represent the homogenized result of damage micromodels and they are obtained through micro-meso relations, which are derived from damage variables and associated forces and which have an intrinsic meaning, being independent of the stacking sequence. The MSD assumes laminates as a stack of homogeneous plies and interfaces, which are considered as mesoconstituents, whose stiffness loss due to the damage is quantified by the variables ρ and τ. The MSD makes the assumption of linear elasticity, therefore it expresses all the involved quantities as the sum of the solution of a problem $\tilde{P}$ in which damage is removed and the solution of a residual problem $\bar{P}$ where a residual stress is applied, correcting the undamaged solution around each damaged area. Accordingly, the homogenized potential energy density of the generic ply ^{S} is expressed as [11]:

$$\frac{2E_p^S}{|S|} = [\pi\bar{\varepsilon}\pi]^t[\bar{M}_1(\bar{I}_{22},\bar{I}_{12})][\pi\bar{\varepsilon}\pi] + \tilde{\sigma}_{33}[\bar{M}_2(\bar{I}_{22},\bar{I}_{12})]\tilde{\sigma}_{33} + \tilde{\sigma}_{33}[\bar{M}_3(\bar{I}_{22},\bar{I}_{12})][\pi\bar{\varepsilon}\pi] - \frac{(1+\bar{I}_{23})\tilde{\sigma}_{23}^2}{\tilde{G}_{23}} - \frac{(1+\bar{I}_{13})\tilde{\sigma}_{13}^2}{\tilde{G}_{23}} - \frac{(1+\bar{I}_{33})<\tilde{\sigma}_{33}^2>_+^2}{\tilde{E}_3} \quad (19)$$

$\bar{I}_{22},\bar{I}_{12},\bar{I}_{23},\bar{I}_{13}$ and $\bar{I}_{33}$ are damage indicators, computed as the integral of the strain energy of the elementary cell for each basic residual problem under the five possible elementary loads in the directions 22, 12, 23, 13, 33.

$[\overline{M}_1]$, $[\overline{M}_2]$, $[\overline{M}_3]$ are operators that depend on the material properties, $|S|$ is the deformation, while $<.>_+$ represents the positive part operator. This relation is "quasi exact", since it disregards the coupling effects, because they are always very small in the practical cases. It features an equivalent state of damage on the mesoscale, which is nearly intrinsic for a given state of microdegradation.

As far as the generic interface $_j$ is concerned, the potential energy density can be written as in [11]:

$$\frac{2E_p^j}{|\gamma_j|} = -\frac{(1+\bar{I}^1)\tilde{\sigma}_{13}}{\tilde{k}_1} - \frac{(1+\bar{I}^2)\tilde{\sigma}_{23}}{\tilde{k}_2} - \frac{(1+\bar{I}^3)\tilde{\sigma}_{33}}{\tilde{k}_3} \tag{20}$$

$\tilde{k}_1$, $\tilde{k}_2$ and $\tilde{k}_3$ are the elastic stiffness coefficients of the interface, $\bar{I}^1$, $\bar{I}^2$ and $\bar{I}^3$ the three damage indicators and γ_j the deformation.

Equations (19) and (20) determine the relationship between the damage indicators and the microdegradation variables ρ and τ of the elementary cell. In fact, they are obtained making the potential energy stored in the plies and in the interfaces the same than in the micromodel. It could be noticed that these equations relate the new elastic properties of the homogenized model to the damage indicators, since the coefficients of the stresses in these relations represent the elastic properties of the homogenized model equivalent to the discretely damaged real model. Therefore a continuum damage model is obtained that is quasi-equivalent from an energy standpoint to the damage micromodel.

Using brick elements to discretize each elementary cell, it is possible to numerically solve the residual problems for determining the damage indicators of Equations (19) and (20). Then, the FD_VK model performs the analysis employing the modified elastic properties given by the mesoscale model, in order to take into consideration the effects of microdamage. Instead of considering the materials healthy as in the unloaded state at the initial iteration, the failure criteria are applied at any time step considering the damage as it is in the reality, since its effects computed at previous iterations are incorporated as modified properties.

In conclusion, the damage growth is described using the initial elastic properties and the stresses that result by this physically based modified expression of the strain energy, instead of simulating damage by guessing appropriate parameters. The stress-based failure criteria used to predict the onset of damage are reported in the Appendix.

The contact problem

As explained in the introductory section, indentation represents for structures a serious design concern, since it can determine the growth of barely visible damage, which may produce a large reduction of their mechanical performance, or even failure.

In the present paper, the indentation depth and the contact area are evaluated assuming the distribution of the contact force to be Hertzian, as customarily. The impactor is described as a rigid body and the effective stiffness of the target structure is simulated by the structural model. The iterative algorithm developed by Palazotto et al. [14] is particularized to the FD_VK model, with the aim of forcing the surface of the target to conform the shape of the impactor, as required by soft structures like sandwiches. At any load increment, an iterative procedure that computes the contact radius (equivalent radius for non-spherical indenter) is repeated till the impactor and the indentation radii are in agreement, then the failure analysis is performed.

At the first instant, the contact force F and the vertical displacement are assumed to be zero. After a small time interval Δt, during which the assumption of no damage is postulated, the contact force becomes $F=\Delta F$ and, according to the Hertzian law, is distributed over the contact area. As a consequence of the applied load $F=\Delta F$, the impactor moves on at a distance influenced by the effective plate stiffness that depends on the plate stiffness and the contact stiffness. The contact radius determines the applied pressure corresponding to the load and it is

computed at every load step using an iterative algorithm that forces the impacted top surface to conform, in the least-squares sense, to the shape of the impactor, applying appropriate constraints. The iterations are repeated till the impactor and the indentation radii are in agreement, then the failure analysis is performed with the damage model described in the previous section. The process is repeated for all the following time steps till the end of the contact time. Since the evaluation of the contact radius at any time step requires very few iterations, this technique gives an accurate description of the contact force and its distribution over the variable contact area not requiring a much larger effort than distributing the contact force over a fixed surface as customarily.

As the solution depends on the current configuration, the previous history and, in addition, deformation can be locally quite large, a modified version of the Newton-Raphson method is adopted to solve the contact problem. The analysis is linearized over any load increment taking into consideration the tangent $[K(q)]_T$ and the secant $[K(q)]_S$ stiffness matrices. The residual force R_i is computed using the secant stiffness matrix, the load at the next iteration $F_{(i)}$ and the solution at the previous iteration $q^0_{(i-1)}$. The tangent stiffness matrix is used to evaluate the updated solution that makes the structure in equilibrium from the residual force balance.

Numerical results

In this section, numerical results obtained using the simulation procedure previously described are compared to experiments dealing with indentation of sandwiches taken from literature. Please note that all the computational times reported in this section refer to analyses performed on a laptop computer with dual-core CPU 2.20 GHz, 64 bit operating system and 4 GB RAM. Finally note that in all the cases, except those by Castanië et al. [35], the analyses by the FD_VK model have been performed considering just a second order expansion for the in-plane displacements and a third order expansion for the transverse displacement, subdividing every physical layer into two computational layers because numerical tests have shown this more efficient for sandwiches than using the approach adopted in the previous work by the authors [9]-[10].

Sandwiches with honeycomb core

First of all, we focus our attention on sandwiches with honeycomb core. As a first test case, let us consider a sandwich with brass faces of 0,1 mm thickness and Nomex™ honeycomb core (HRH78, 1/8, 3) of 15 mm thickness. Castanië et al. [35] presented experimental and numerical results of quasi-static indentation tests carried out on 100x100mm fully supported sandwiches. The indentations tests were carried out using spherical indenters with radii of 21,75, 30,125 and 57,25 mm. The numerical results by Castanië et al. [35] were obtained using a nonlinear finite element model. An elastic modulus of 103100 MPa and a yield stress of 433 MPa were assumed for the brass faces. The honeycomb core was simulated with nonlinear spring, placed at the same location as the honeycomb cell angles and the faces with Mindlin plate element. From Figure 3 it could be noticed that the results by the present simulation procedure are in accordance with the numerical and experimental ones by Castanië et al. [35]. It could be underlined that our finite element analysis calls for 20 elements across the thickness of the honeycomb, while, as far as the mesoscale model is concerned, the reduction of the mechanical properties of the core is influenced by the indenter radius. Specifically a 30% reduction is necessary, for the smallest indenter, a 33% reduction is required by the indenter with 30,125 mm radius and in the last case a 37% reduction is needed. The computational time is no longer affected by the indenter dimension, since in all the cases the analysis takes about 39 s.

Castanië at al. [35] showed also the experimental and numerical results for another sandwich plate with honeycomb core. As in the previous case, the plate is fully supported, it is square with a 100 mm side and the Nomex™ honeycomb core (HRH78, 1/8, 3) is 15 mm thick. The plates has brass faces of 1 mm thickness and according to Castanië et al. [35], the elastic modulus of the brass is 70400 MPa, its yield stress is 104 MPa. Once again, the indentations are carried out using spherical indenters with radii of 21,75, 30,125 and 57,25 mm. As in the previous case, the numerical results by the current simulation procedure are in good agreement with those presented by Castanië et al. [35], as shown by Figure 4. During the finite element analysis 20 elements across the thickness of the honeycomb are again required, and, also in this case the indenter size has a bearing in determining the results by the mesoscale model. In fact the first indenter calls for a 27% reduction of the mechanical of the core, while 29% and 35% reductions are required in the other cases. As far as computational burden is concerned, nearly 43 s are required in the three cases.

As already mentioned, the numerical results of Figure 3 and 4 by the FD_VK model are obtained using a representation, which is different from that adopted in the following cases. Specifically in-plane displacements and transverse displacement of the faces are represented using a second order expansion, while a third order expansion of the transverse displacement and a second order expansion of in-plane displacements are adopted across the core. A single computational layer is considered for each physical layer.

Now we consider sandwiches with laminated faces. We investigate the cases analysed by Williamson and Lagace [36] that presented experimental indentation curves for a rigidly supported sandwich plate indented by a 25,4 mm diameter hemispherical nose. The faces are 3,25 mm thick and they are realized with AS4/3501-6 carbon/epoxy prepregs, whose mechanical properties are E_{11}= 142 GPa, E_{22}= 9,8 GPa, G_{12}= 7,1 GPa, υ_{12}=0,3. The 25,4 mm thick core is in HRH 10 1/8-3,0 Nomex^{TM} honeycomb. The comparison between experimental and numerical results is reported in Figure 5, where also the numerical results by Hoo Fatt and Park [37] are considered. They were obtained using the principle of minimum potential energy. Differently to what done in this paper, Hoo Fatt and Park [37] did not consider the contact problem to be Hertzian, as they supposed that the top face sheet is resting on a deformable plastic foundation (an elastic, perfectly plastic core hypothesis).

The finite element analysis needs 30 elements across the thickness of the core, while the mesoscale model calls for a 36% reduction of the mechanical properties of the core and a 41% reduction of those of the faces. As far as computational times are concerned, the analysis takes 50 s.

Williamson and Lagace [36] presented experimental load indentation curve also for a simply supported sandwich plate with multilayered faces. As in the previous case, the plate is indented by a 25,4 mm diameter hemispherical nose. The faces are 2 mm thick and they are realized with AS4/3501-6 graphite-epoxy laminate, whose mechanical properties are E_{11}= 144,8 GPa, E_{22}= 9,7 GPa, G_{12}= 7,1 GPa, υ_{12}=0,3. The 12,7 mm thick core is in HRH 10 1/8-4,0 Nomex^{TM} honeycomb. The stacking sequence is $[0°/\ 90°/\ 0°/\ 90°/\ 0°/\ 90°\ /\ 0°\ /\ 90°/\ 0°/\ 90°/\ 0°/\ 90°/\ 0°/\ 90°/\ 0°/\ 90°/\ \text{core}]_s$.

The results by the present simulation procedure are shown in Figure 6, where they are compared with those by Williamson and Lagace [36] and by Hoo Fatt and Park [37]. In this case the finite element analysis calls for 15 elements across the thickness, while the mesoscale model provides a 38% reduction of the mechanical properties of the core and a 42% reduction of those of the faces. The presence of multilayered faces determines an increase of the computational times, which for this case is 55 s.

Foamed core sandwiches

As final example, let us consider the sandwich panel with foam core analysed by Potluri et al. [38]. The panel is square with a 300 mm side and it is clamped. Its faces are in woven glass fabric of weight 600 g/m^2, while the core is in Divinycell H130. The face thickness is 1 mm and the core is 25 mm thick. Indentation is carried out with a 25 mm flat-faced indenter.

The results presented in Figure 7 are in good agreement with the experiments by Potluri et al. [38]. Please note that in this case 30 solid elements across the thickness have been considered in order to get an evaluation of the crushing behaviour of the Divinycell core. The mesoscale model calls for a 41% reduction of the mechanical properties of the upper face and a 37% reduction of those of the core. The computational time required by this analysis is 45 s.

As a general conclusion it could be noticed that in all the sample cases the simulation procedure presented provides results in good agreement with experimental ones. However, at the same time, the computational times reported for each case are very low, since the most intricate analysis takes only 55 s. This achievement is reached primarily thanks to the efficiency of the FD_VK, but also the MSD model and the choice of carrying apart the evaluation of the core crushing behaviour play an important role in this context. These features make the present simulation procedure suited for the analysis of structures of industrial complexity.

Concluding remarks

Indentation of sandwiches with honeycomb or foam core has been investigated using a recently developed zig-

zag model with variable kinematics, together with mesoscale damage model. The paper is aimed at developing a modelling approach able to reduce the computational burden with respect to the typical procedure. Sandwiches are treated as multi-layered composites, whose properties vary with the applied load. The core crushing behaviour is determined apart once at a time using finite element analysis. Once the properties of the core have been determined, the analysis is carried out in closed form using the adaptive model by the authors. It has a variable kinematics, but only five degrees of freedom, in order to keep as low as possible the computational effort. The damage formation is determined using stress-based criteria, as customarily, while the damage growth is accurately and efficiently taken into consideration employing a mesoscale model. The present simulation procedure provides results in good agreement with experiments, in all the cases examined. At the same time the computational effort is kept also very low because the evaluation of the variable elastic properties of the core is carried out apart once at a time. In details, the analysis of the most complex case considered (a sandwich panels with 32 layers) takes only 55 s, therefore the present simulation procedure is suited to analyse structures of industrial complexity..

References

[1] Daniel IM and Ishai O. Engineering mechanics of composite materials. 2nd Ed. Oxford: University Press, 2005.
[2] Davies GAO, Hitchings D and Ankersen J. Predicting delamination and debonding in modern aerospace composite structures. Comp Sci Tech 2006; 66: 846-854.
[3] De Freitas M, Silva A and Reis L. Numerical evaluation of failure mechanisms on composite specimens subjected to impact loading. Comp Part B 2000; 31: 199-207.
[4] Wang SX, Wu LZ and Ma L. Low-velocity impact and residual tensile strength analysis to carbon fiber composite laminates. Materials & Design 2010; 31: 118-125.
[5] Borg R, Nilsson L and Simonsson K. Simulation of low velocity impact on fiber laminates using a cohesive zone based delamination model. Compos Sci Tech 2004; 64: 279-288.
[6] Nishikawa M, Okabe T and Takeda N. Numerical simulation of interlaminar damage propagation in CFRP cross-ply laminates under transverse loading, Int J of Solids & Struct 2007; 44: 3101-3113.
[7] Diaz-Diaz A, Caron JF and Ehrlacher A. Analytical determination of the modes I, II and III energy release rates in a delaminated laminate and validation of a delamination criterion. Comp Struct 2007; 78: 424-432.
[8] Qiao P and Yang M. Impact analysis of fiber reinforced polymer honeycomb composite sandwich beams. Comp Part B 2007; 38: 739-750.
[9] Icardi U and Sola F. Development of an efficient zigzag model with variable representation of displacements across the thickness. J Eng Mech (In press).
[10] Icardi U and Sola F. Recovering critical stresses in sandwiches using through-the-thickness reinforcement, Comp Part B. Epub ahead of print 1 June 2013. DOI: http://dx.doi.org/10.1016/j.compositesb.2013.05.027.
[11] Ladevèze P and Lubineau G. On a damage mesomodel for laminates: micromechanics basis and improvement. Mech of Materials 2003; 35: 763-775.
[12] Ladevèze P, Lubineau G and Marsal D. Towards a bridge between the micro- and mesomechanics of delamination for laminated composites. Comp Sci Tech 2006; 66: 698-712.
[13] McQuigg TD. Compression After Impact experiments and analysis on honeycomb core sandwich panels with thin face sheets. Report no. NASA/CR–2011-217157, NASA Langley Research Center Hampton, USA, 2011.
[14] Palazotto AN, Herup EJ and Gummadi LNB. Finite element analysis of low-velocity impact on composite sandwich plate. Comp Struct 2000; 49: 209-227.
[15] Zhang Y and Yang C. Recent developments in finite element analysis for laminated composite plates. Comp Struct 2009; 88: 147-157.
[16] Moreira RAS and Rodrigues JD. A layerwise model for thin soft core sandwich plates. Comput & Struct 2006; 84: 1256-1263.
[17] Chrysochoidis NA and Saravanos DA. Generalized layerwise mechanics for the static and modal response of delaminated composite beams with active piezoelectric sensors. Int J of Solids & Struct 2007; 44: 8751-8768.
[18] Hohe J and Librescu L. Recent results on the effect of the transverse core compressibility on the static

and dynamic response of sandwich structures. Comp Part B 2008; 39: 108-119.
[19] Shariyat M. A Generalized high-order global-local plate theory for nonlinear bending and buckling analyses of imperfect sandwich plates subjected to thermo-mechanical loads. Comp Struct 2010; 92: 130–143.
[20] Zhen W and Wanji C. An assessment of several displacement-based theories for the vibration and stability analysis of laminated composites and sandwich beams. Comp Struct 2008; 84: 337–349.
[21] Icardi U and Ferrero L. Impact analysis of sandwich composites based on a refined plate element with strain energy updating. Comp Struct 2009; 89: 35-51.
[22] Ramtekkar GS, Desai YM and Shah AH. Application of a three-dimensional mixed finite element model to the flexure of sandwich plate. Comput & Struct 2003; 81: 2183–2198.
[23] Chia CY. Nonlinear analysis of plates. New York: McGraw-Hill International Book Company, 1980
[24] Mohmmed R, Zhang F, Sun B and Gu B. Finite element analyses of low-velocity impact damage of foam sandwiched composites with different ply angles face sheets. Materials & Design 2013; 47: 189-199.
[25] Aminanda Y, Castaniè B, Barrau JJ and Thevenet P. Experimental analysis and modeling of the crushing of honeycomb cores. Appl Compos Mater 2005; 12: 213-227.
[26] Aktay L, Johnson AF and Kröplin B. Numerical modeling of honeycomb core crush behavior Eng Fracture Mech 2008; 75: 2616-2630.
[27] Flores-Johnson EA, Li QM and Mines RAW. Degradation of elastic modulus of progressively crushable foams in uniaxial compression. J of Cellular Plastics 2008; 44: 415-434.
[28] Ivañez I, Santiuste C and Sanchez-Saez S. FEM analysis of dynamic flexural behaviour of composite sandwiches beams with foam core. Comp Struct 2010; 92: 2285-2291.
[29] Gibson LJ and Ashby MF. Cellular solids. Oxford: Pergamon, 1988
[30] Bathe KJ. Finite element procedures. Englewood Cliffs: Prentice-Hall, 1996.
[31] Lee SM and Tsotsis TK. Indentation failure behaviour of honeycomb sandwich panels. Comp Sci & Tech 2000; 60: 1147–1159.
[32] Petras A and Sutcliffe MPF. Indentation resistance of sandwich beams. Comp Struct 1999; 46: 413–424.
[33] Besant T, Davies GAO and Hitchings D. Finite element modelling of low velocity impact of composite sandwich panels. Comp Part A 2001; 32: 1189-1196.
[34] Koissin V, Shipsha A and Skvortsov V. Wrinkling in sandwich panels - an analytical approach. J Sandwich Struct & Mat 2011; 13: 705-730.
[35] Castaniè B, Bouvet C, Aminanda Y, Barrau JJ and Thevenet P. Modelling of low-energy/low-velocity impact on Nomex honeycomb sandwich structures with metallic skins. Int J Impact Eng 2008; 35: 620-634.
[36] Williamson JE and Lagace PA. Response mechanism in the impact of graphite/epoxy honeycomb sandwich panels. In: Eighth ASC Technical Conference, Cleveland, OH, 1993, pp. 287-297.
[37] Hoo Fatt MS and Park KS. Dynamic models for low-velocity impact damage of composite sandwich panels – Part A: Deformation. Comp Struct 2001; 52: 335-351.
[38] Potluri P, Kusak E and Reddy TY. Novel stitch-bonded sandwich composite structures. Comp Struct 2003; 59: 251-259.

Appendix

It is well known that, in order to get a truthful estimation of the onset of damage, the failure criteria should consider the transverse tensile compressive stress independently of other stresses. In addition, continuous stiffness degradation together with the specific inter fibre fracture mode should be accounted for. Accordingly, in this paper, stress-based criteria with a separate description of the various failure modes are adopted to describe the onset of damage, since they are simple enough for a computational efficient implementation and quite accurate.

The fibre's failure and the failure of the matrix are predicted using the 3-D Hashin's criterion with *in-situ* strengths. Therefore tensile failure of fibres occurs if:

ISSN: 2349-5197
Impact Factor: 2.715

INTERNATIONAL JOURNAL OF RESEARCH SCIENCE & MANAGEMENT

$$\left(\frac{\sigma_{11}}{X^t}\right)^2+\frac{1}{S_{12=13}{}^2}\left(\tau_{12}{}^2+\tau_{13}{}^2\right)=1,\ (\sigma_{11}>0) \qquad \text{(A-1)}$$

$S_{12=13}$ is the *in-situ* shear strength of the resin, X^t the tensile strength of fibres and σ_{11}, τ_{12}, τ_{13} the tensile and shear stresses acting on the fibres. Compressive failure of fibres is predicted to occur if:

$$\sigma_{11}=-X^c,\ (\sigma_{11}<0) \qquad \text{(A-2)}$$

Where X^c represents the compressive strength of fibres. Matrix failure under traction is expected to arise if:

$$\left(\frac{\sigma_{22}+\sigma_{33}}{Y^t}\right)^2+\frac{1}{S_{23}{}^2}(\tau_{23}{}^2-\sigma_{22}\sigma_{33})+\left(\frac{\tau_{12}}{S_{12=13}}\right)^2+\left(\frac{\tau_{13}}{S_{12=13}}\right)^2=1\ (\sigma_{22}+\sigma_{33}>0) \qquad \text{(A-3)}$$

while under compression, matrix failure occurs if:

$$\frac{1}{Y^c}\left[\left(\frac{Y^c}{2S_{23}}\right)^2-1\right](\sigma_{22}+\sigma_{33})+\frac{(\sigma_{22}+\sigma_{33})^2}{4S_{23}{}^2}+\frac{(\tau_{23}{}^2-\sigma_{22}\sigma_{33})}{S_{23}{}^2}+\frac{(\tau_{12}{}^2+\tau_{13}{}^2)}{S_{12=13}{}^2}=1 \qquad \text{(A-4)}$$

$$(\sigma_{22}+\sigma_{33}<0)$$

The onset of delamination is predicted using the Choi-Chang's criterion, since as shown by many researchers it gives accurate estimations. Delamination is predicted to start if

$$e_d^2=D_a\left[\frac{\bar{\sigma}_{yz}^n}{S_i^n}+\frac{\bar{\sigma}_{xz}^{n+1}}{S_i^{n+1}}+\frac{\bar{\sigma}_{yy}^{n+1}}{Y_i^{n+1}}\right]^2>1 \qquad \text{(A-5)}$$

where $Y^{n+1}=Y_t^{n+1}$ if $\bar{\sigma}_{yy}\geq 0$, or $Y^{n+1}=Y_c^{n+1}$ if $\bar{\sigma}_{yy}<0$, D_a is an empirical constant that is defined after consideration of the material properties, $\bar{\sigma}_{ij}$, which is the average stress at the interface between the n^{th} ply and the $n+1^{\text{th}}$ ply, is computed as follows:

$$\bar{\sigma}_{ij}^{n+1}=\frac{1}{h_{n+1}}\int_{t_{n-1}}^{t_n}\sigma_{ij}dt \qquad \text{(A-6)}$$

The subscript *'i'* stands for *in-situ*, while *'t'* and '*c*' stand for traction and compression, respectively. This criterion does not take into consideration the transverse interlaminar stress σ_{33}. However numerical tests in literature have shown that, in the majority of cases, this component has not a significant bearing.
The criterion by Besant et al. [33] is chosen to predict the failure of sandwiches with honeycomb core under compression and transverse shear. Failure occurs when:

$$\left(\frac{\sigma_{zz}}{\sigma_{cu}}\right)^n+\left(\frac{\tau_{xz}}{\tau_{lu}}\right)^n+\left(\frac{\tau_{yz}}{\tau_{lu}}\right)^n>1 \qquad \text{(A-7)}$$

σ_{cu} and τ_{lu} are the core strengths in compression and transverse shear. In this paper, it is chosen n= 1,5, because this value best fitted the experimental results. Nevertheless numerical tests in literature have shown that varying the exponent from 1 to 2 does not determine any remarkable effects on the results of sandwiches with laminated faces.

ISSN: 2349-5197
Impact Factor: 2.715

INTERNATIONAL JOURNAL OF RESEARCH SCIENCE & MANAGEMENT

The rule suggested by Evonik for Rohacell core is used to predict the failure of foam cores:

$$\sigma_v = \frac{\sqrt{(12a_2 + 12a1 + 12)I_2 + [4a_2{}^2 + (4a_1 + 4)a_2 + a_1{}^2]I_1{}^2} + a_1 I_1}{2a_2 + 2a_1 + 2} \quad \text{(A-8)}$$

$$where \quad I_1 = \sigma_{11} + \sigma_{22} + \sigma_{33}$$

$$and \; I_2 = \frac{1}{3}\left[\sigma_{11}{}^2 + \sigma_{22}{}^2 + \sigma_{33}{}^2 - \sigma_{11}\sigma_{22} - \sigma_{11}\sigma_{33} - \sigma_{22}\sigma_{33} + 3(\sigma_{12}{}^2 + \sigma_{13}{}^2 + \sigma_{23}{}^2)\right]$$

Using as safety factor R_{11}/σ_v. The empiric parameters $a_1 = k^2(d-1)/d$, $d = R_{11}^-/R_{11}^+$, $a_2 = (k^2/d) - 1$ and $k = \sqrt{3}R_{12}/R_{11}^+$ are determined from experiments, R_{11}^+, R_{11}^- and R_{12} are the strengths of the foam under traction compression and shear, respectively.

The criteria by Lee and Tsotsis [31] and Petras and Sutcliffe [32] are adopted to estimate failure indentation due to core crushing under out-of-plane normal and shear stresses. The former predicts indentation failure to occur when one of these inequalities is verified:

$$\frac{\sigma_{zz}}{Z^c} = 1 \;,\; \frac{\sigma_{xz}}{S^x} = 1 \;,\; \frac{\sigma_{yz}}{S^y} = 1 \quad \text{(A-9)}$$

Z^c, S^x, S^y are the compressive yield strength and the out-of-plane shear strengths, respectively. The loading amplitude is set as the failure load once an inequality is satisfied. The latter predicts indentation failure when:

$$\frac{\sigma_{zz}}{Z^c} + \frac{(\sigma_{xz} + \sigma_{yz})}{S} = 1 \quad \text{(A-10)}$$

S is the transverse shear strength.

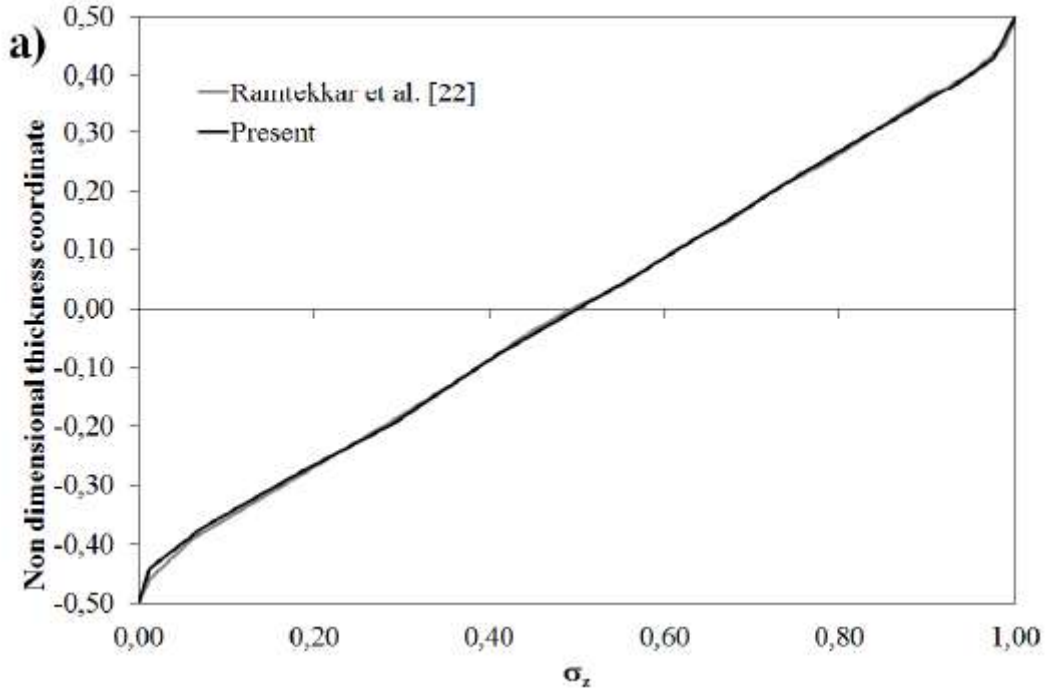

Figure 1a

ISSN: 2349-5197
Impact Factor: 2.715

INTERNATIONAL JOURNAL OF RESEARCH SCIENCE & MANAGEMENT

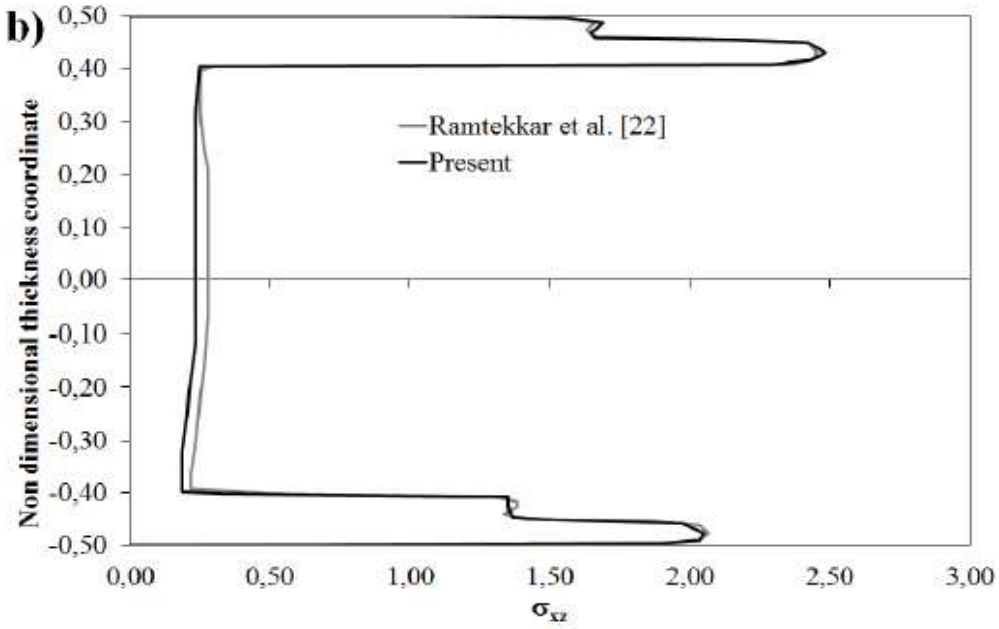

Figure 1b

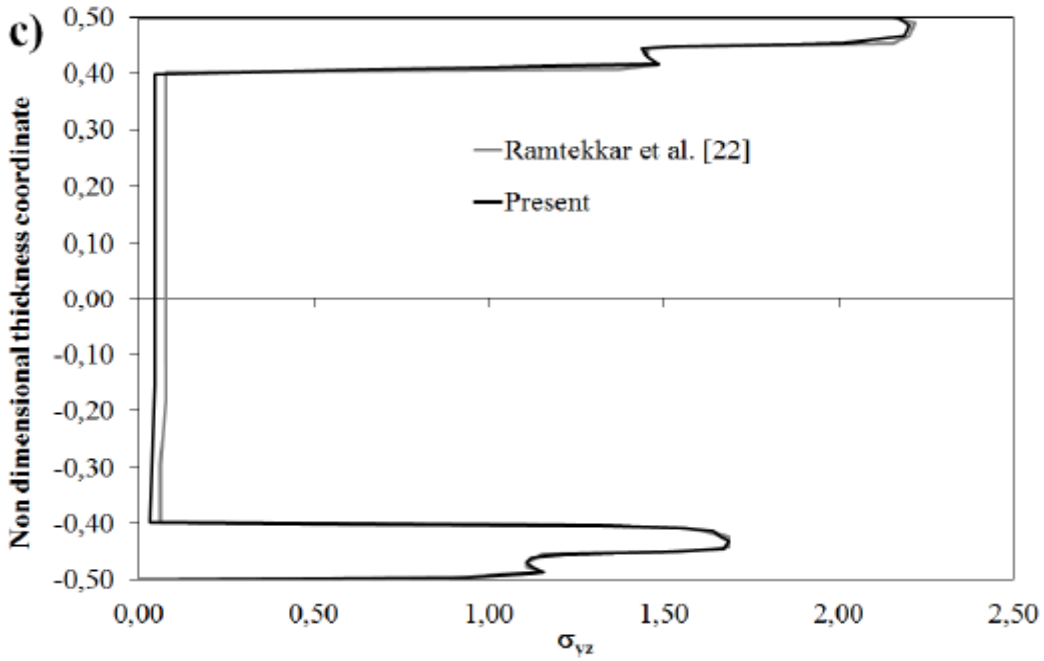

Figure 1c

Figure 1. Through-the-thickness distribution of a) transverse normal stress σz, transverse shear stress b) σxz and c) σyz by the FD_VK model and by Ramtekkar et al. [22].

ISSN: 2349-5197
Impact Factor: 2.715

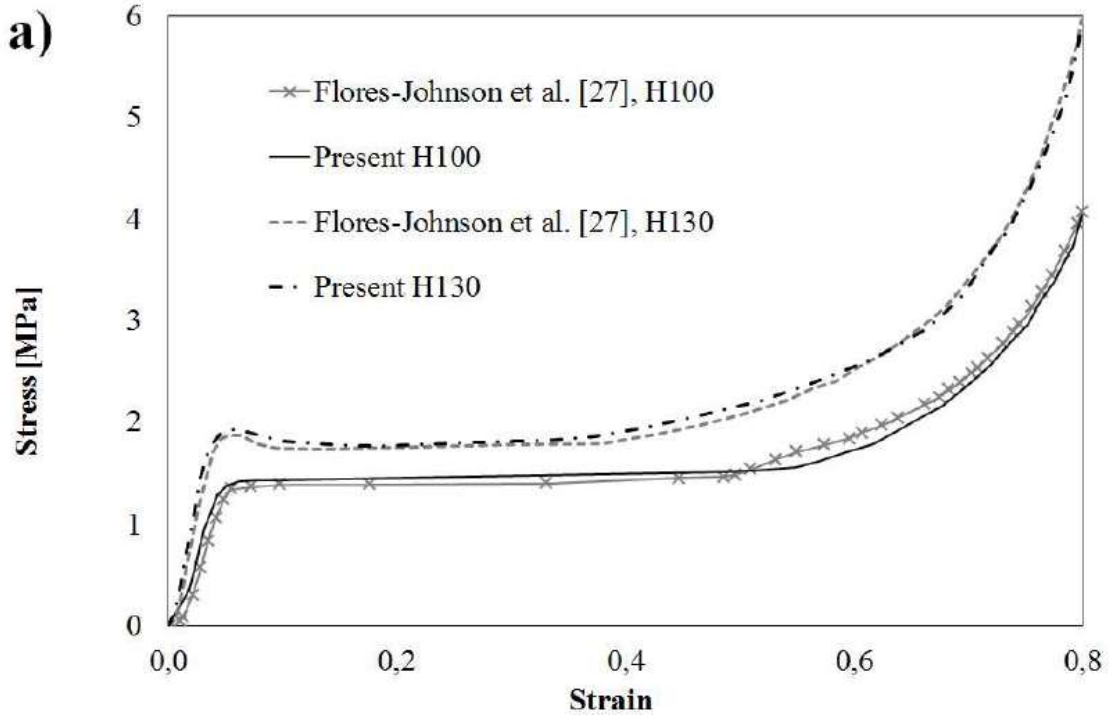

Figure 2a

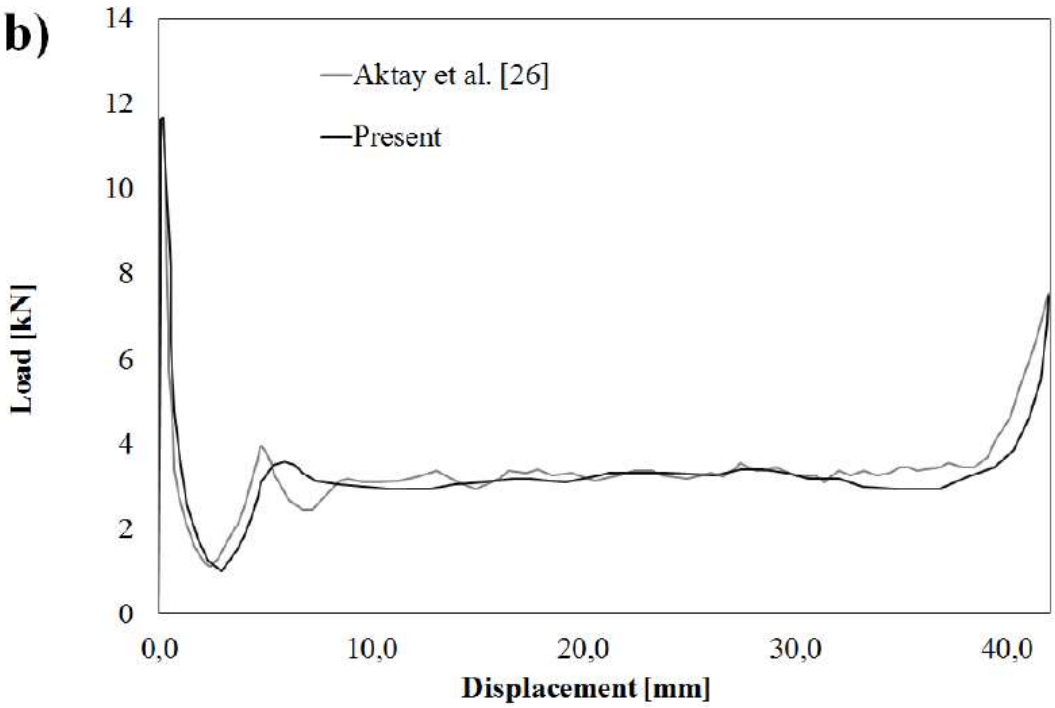

Figure 2b

Figure 2. Comparison between experimental and numerical crushing behaviour for sandwiches with a) foam core (Divinycell H100 and H130) and b) 5052 aluminium honeycomb

ISSN: 2349-5197
Impact Factor: 2.715

INTERNATIONAL JOURNAL OF RESEARCH SCIENCE & MANAGEMENT

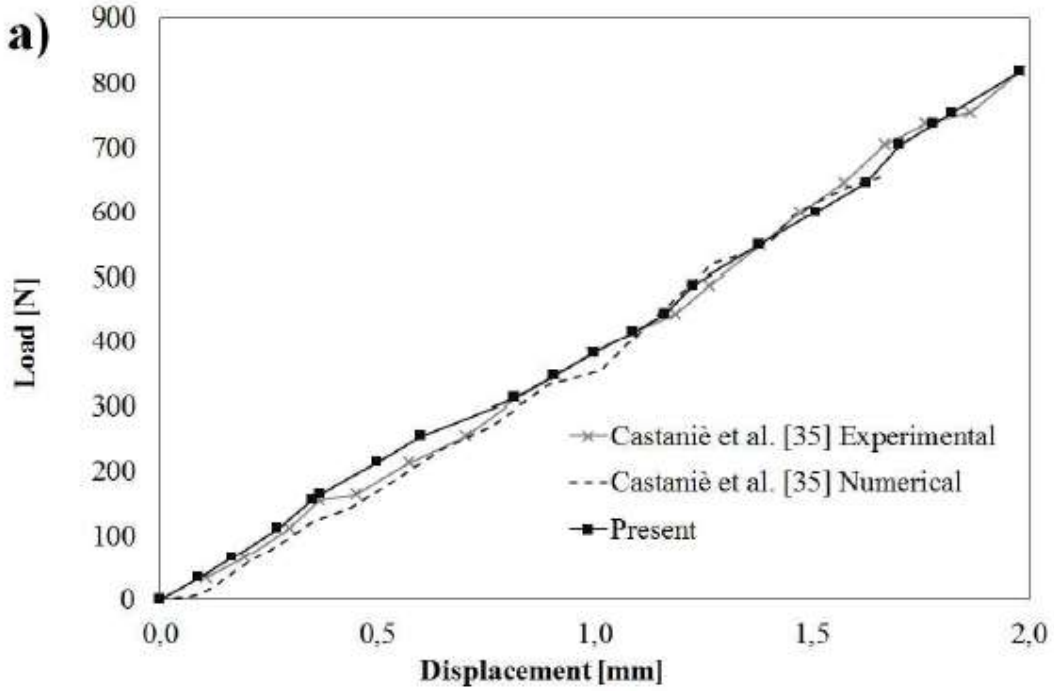

Figure 3a

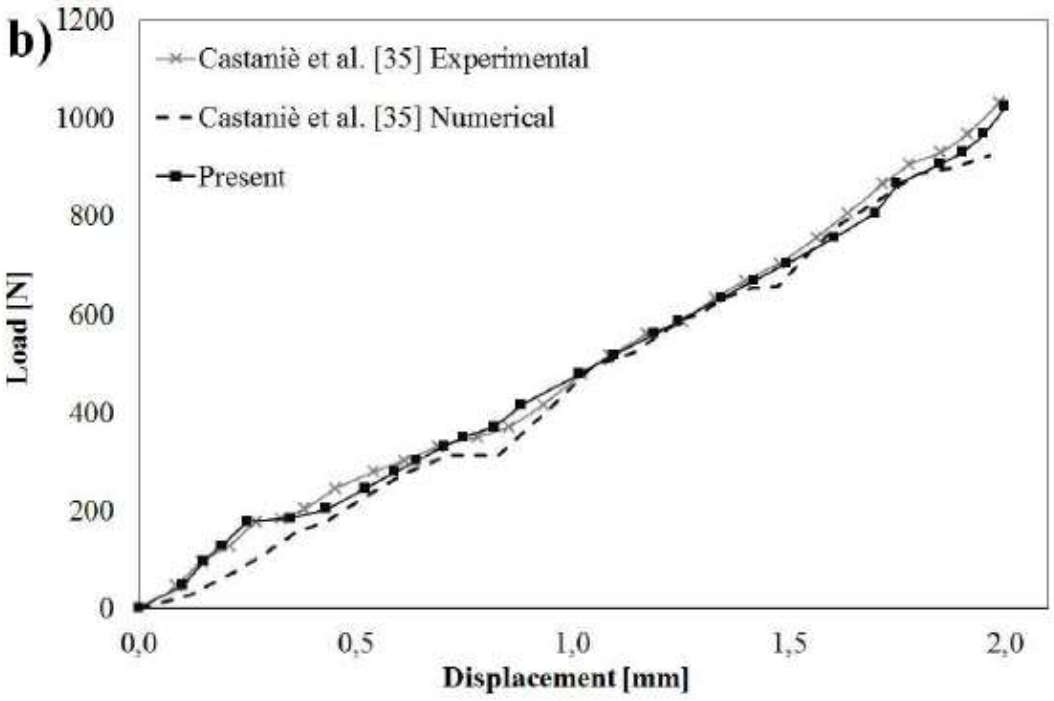

Figure 3b

ISSN: 2349-5197
Impact Factor: 2.715

INTERNATIONAL JOURNAL OF RESEARCH SCIENCE & MANAGEMENT

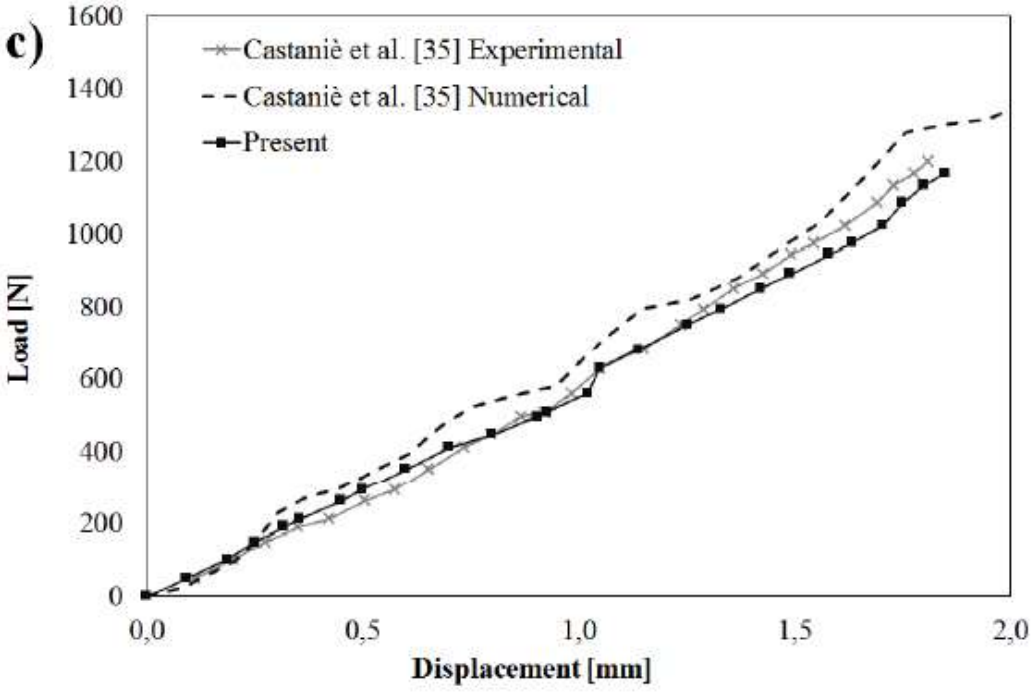

Figure 3c

Figure 3. Comparison between experimental and numerical force-indentation curves for a fully supported NomexTM honeycomb sandwich with thin brass faces (thickness 0,1 mm), stricken by an indenter with radius of a) 21,75 mm, b) 30,125 and c) 57,25 mm.

ISSN: 2349-5197
Impact Factor: 2.715

INTERNATIONAL JOURNAL OF RESEARCH SCIENCE & MANAGEMENT

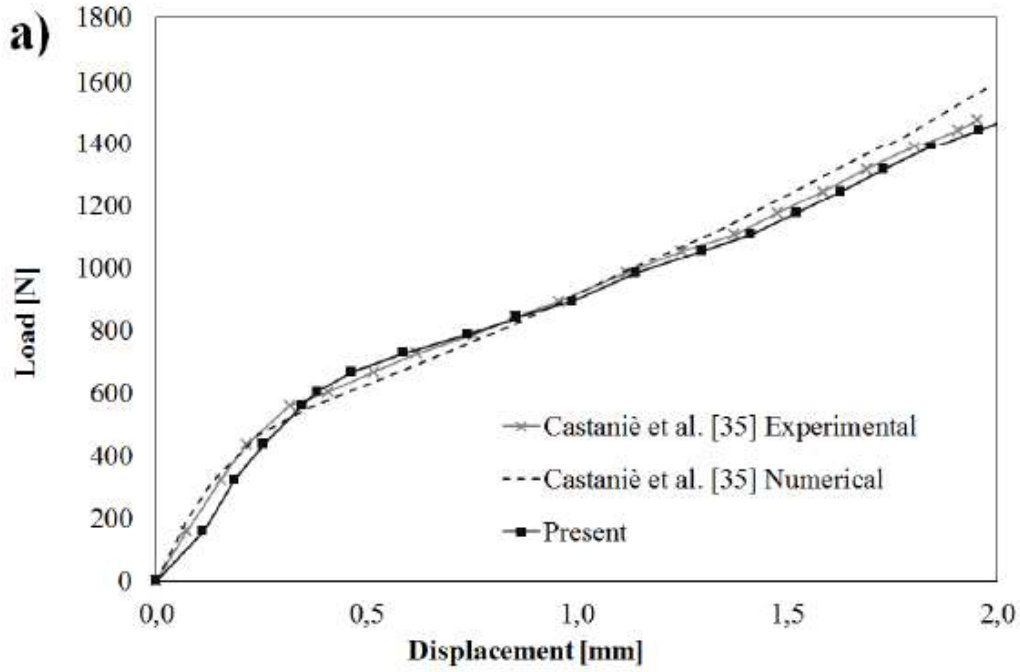

Figure 4a

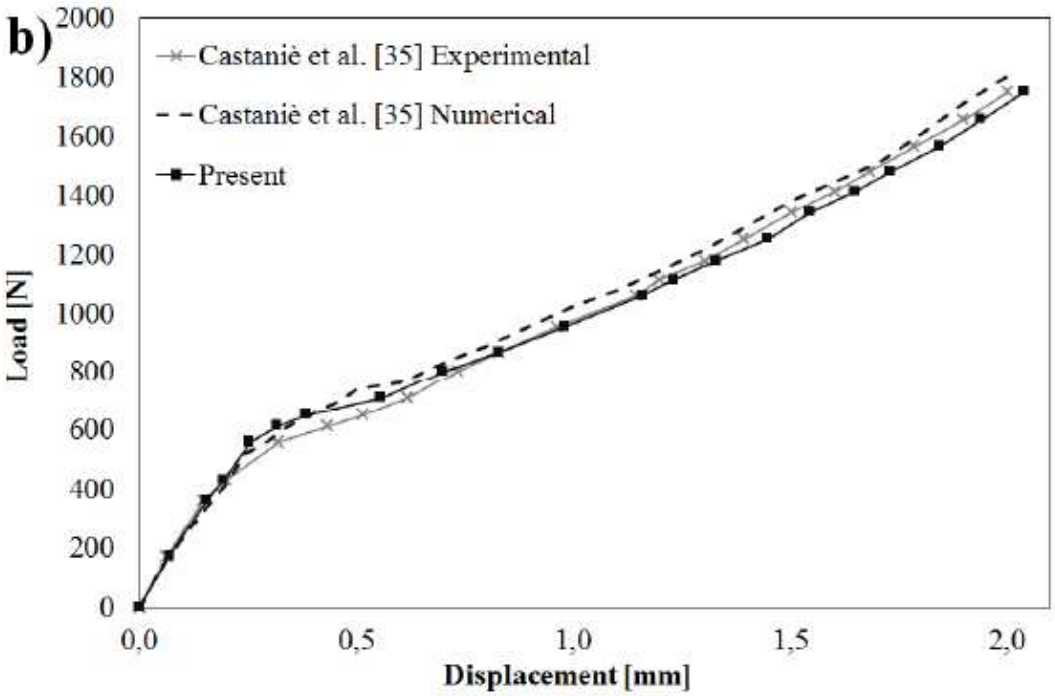

Figure 4b

ISSN: 2349-5197
Impact Factor: 2.715

INTERNATIONAL JOURNAL OF RESEARCH SCIENCE & MANAGEMENT

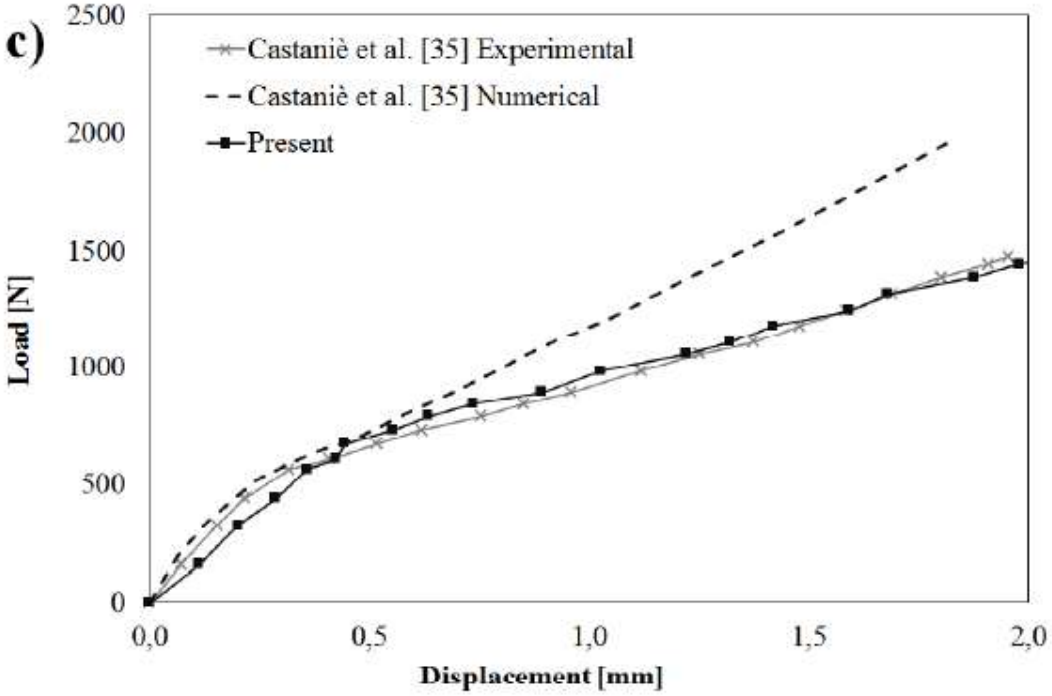

Figure 4c

Figure 4. Comparison between experimental and numerical force-indentation curves for a fully supported NomexTM honeycomb sandwich with thick brass faces (thickness 1 mm), stricken by an indenter with radius of a) 21,75 mm, b) 30,125 and c) 57,25 mm.

ISSN: 2349-5197
Impact Factor: 2.715

INTERNATIONAL JOURNAL OF RESEARCH SCIENCE & MANAGEMENT

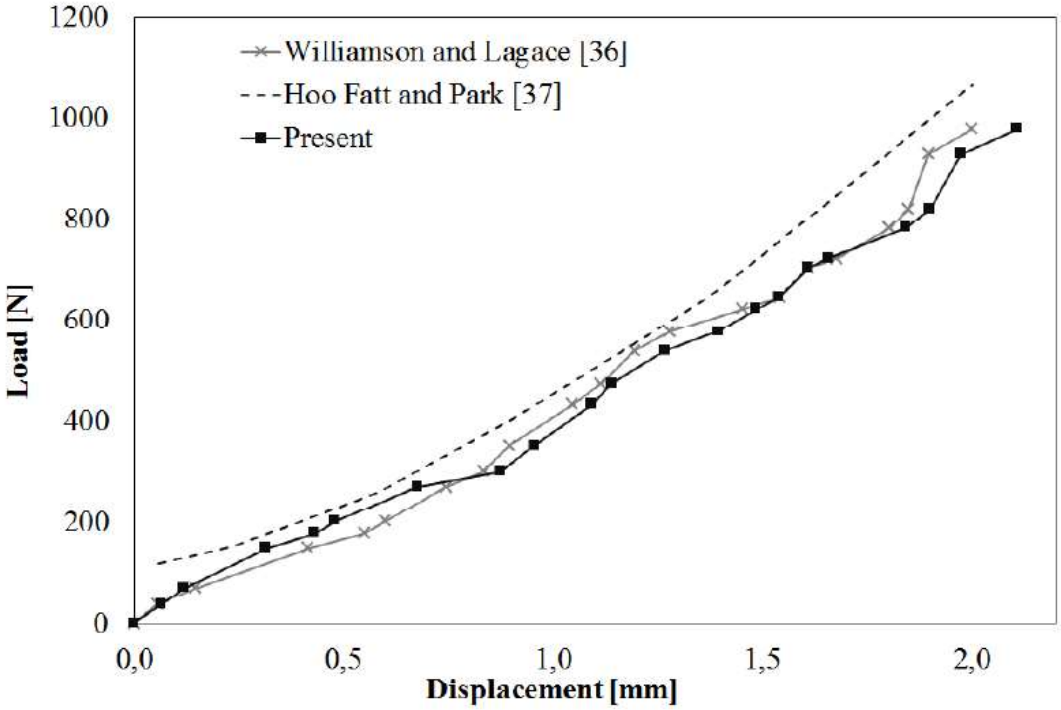

Figure 5. Comparison between experimental and numerical force-indentation curves for a rigidly supported NomexTM honeycomb sandwich plate indented by a 25,4 mm diameter hemispherical nose.

ISSN: 2349-5197
Impact Factor: 2.715

INTERNATIONAL JOURNAL OF RESEARCH SCIENCE & MANAGEMENT

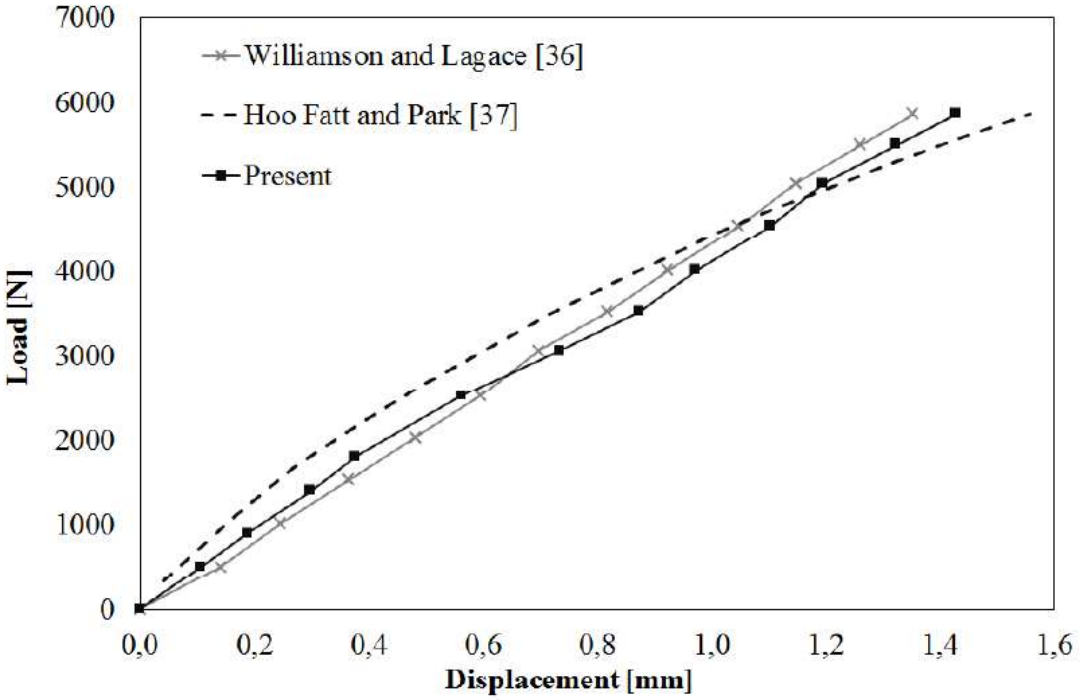

Figure 6. Comparison between experimental and numerical force-indentation curves for a rigidly supported NomexTM honeycomb sandwich plate with multilayered faces indented by a 25,4 mm diameter hemispherical nose.

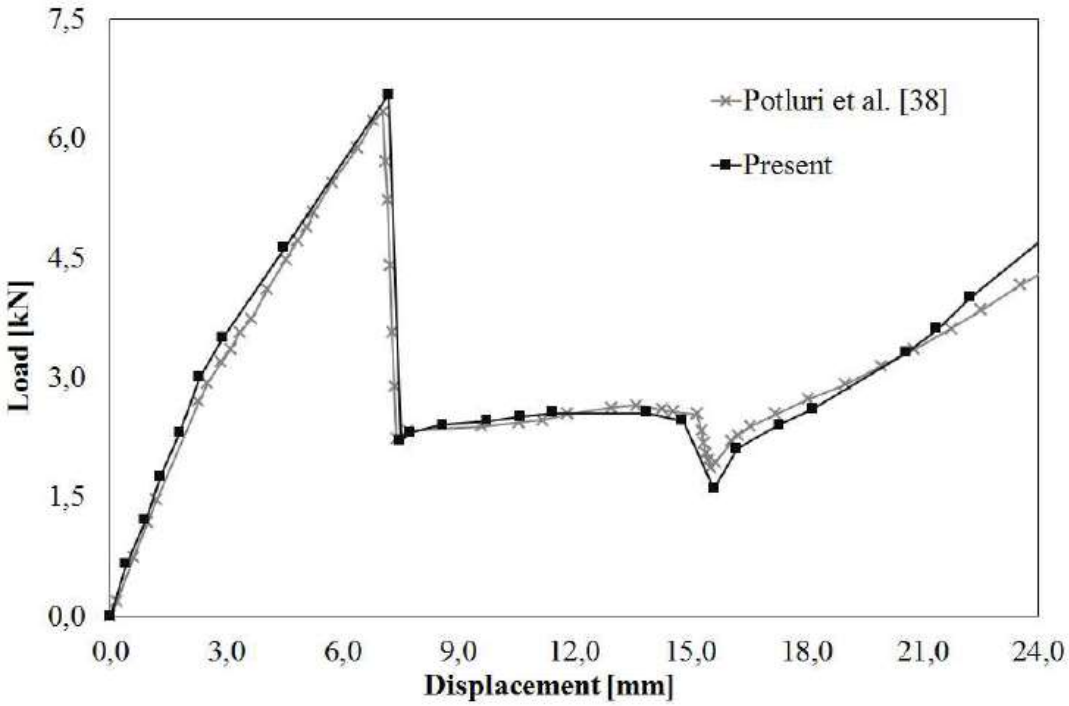

Figure 7. Comparison between experimental and present numerical force–indentation curves for a clamped sandwich panel with Divinycell H130 foam core indented by a 25 mm flat-faced indenter